Nano-Arrayed OLEDs: Enhanced Outcoupling Efficiency and Suppressed Efficiency Roll-Off (Electronic Supplementary Information)

Ha Hwang[1], Yong Sub Shim[1], Junhee Choi[1], Dong Jun Lee[1], Jae Geun Kim[1], Ju Sung Lee[1], Young Wook Park[2] and Byeong-Kwon Ju[1*]*

[1] Display and Nanosystem Laboratory, College of Engineering, Korea University, 145 Anam-ro, Seongbuk-gu, Seoul 02841, Republic of Korea

[2] School of Mechanical and ICT Convergence Engineering, Sun Moon University, Choongcheongnamdo 31460, Republic of Korea

***To whom correspondence should be addressed.**

E-mail: bkju@korea.ac.kr (B.K.J.); zerook@sunmoon.ac.kr (Y.W.P.)

Keywords

Organic light-emitting diodes (OLEDs), Surface Plasmon, Nanosize pixel defining layer (nPDL), Laser interference lithography (LIL), Finite-difference time domain (FDTD) simulation

1. Light extraction efficiency according to taper angle

In the FDTD simulation data shown in **Figure S1a, b**, the optical-enhancement factor depends on the taper angle of the diffraction grating at the metal-organic interface. The enhancement factor significantly decreases when the taper angle of the diffraction grating is 90 degree. On the other hand, the diffraction grating with the taper angle of 45 degree shows the maximum enhancement factor for nano-arrayed OLEDs with the FF of 0.25.

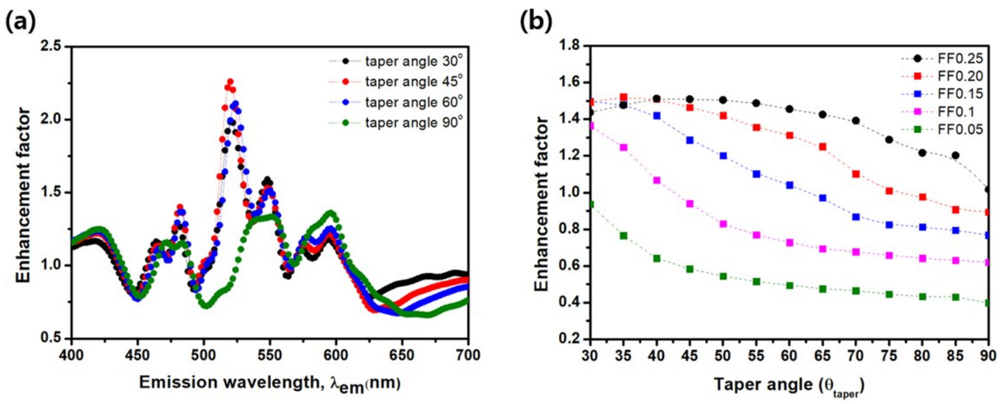

Figure S1. (a) Enhancement factor-emission wavelength graph with respect to the taper angle of the diffraction grating. (b) Enhancement factor with respect to the taper angle in the green FWHM bandwidth range (495-550nm).

Figure S2 shows far-filed intensity distribution of nano-arrayed OLEDs with the taper angle of 45 degree and 90 degree. The SPP diffraction pattern is strongly observed in the Figure S2a than Figure S2b in the green emission region, which indicates that the wavy diffraction grating with the taper angle of 45 degree shows the higher enhancement of the optical efficiency than the diffraction grating with the taper angle of 90 degree.

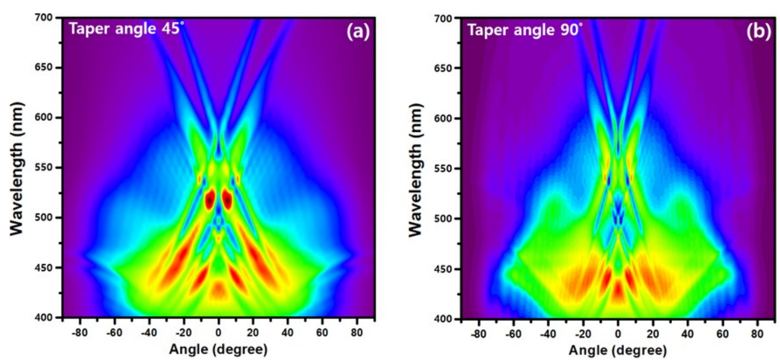

Figure S2. Far-field intensity angular distribution of nano-arrayed OLEDs with the taper angle of (a) 45 degree (b) 90 degree.

2. Nano-optics of the nPDL

The nPDL structure contributes to the optical efficiency in two ways, as shown in **Figure S3**.

(1) The PC effect between the nPDL and the organic layer;

(2) The reduced SPP loss at the metal–organic interface.

To investigate these nano-optical effects of the nPDL, nano-arrayed OLEDs with pitches of 310 nm, a height of 35 nm, and an FF of 0.25 were analyzed via FDTD simulation.

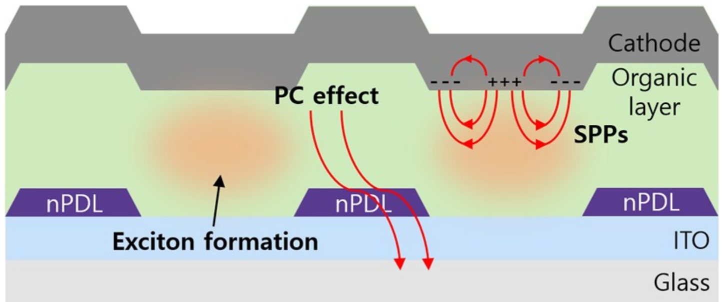

Figure S3. Nano-optical effect of the nPDL in the nano-arrayed OLEDs: (1) PC effect, (2) SPP loss.

2-1. PC effect

The PC effect is maximized when the refractive indices of the two materials forming the PC structure differ significantly. To investigate the PC effect in the nano-arrayed OLEDs, the refractive indices of the organic layer and the nPDL were measured using the thin-film analyzer.

As shown in **Figure S4a**, the PC effect of the nPDL on the optical efficiency is negligible because the difference in the refractive indices between nPDL and organic materials is very small in the visible-wavelength range. Thus, the simulation data show almost the same enhancement factor regardless of the presence of the nPDL, as shown in **Figure S4b**.

On the other hand, a greater difference in the refractive indices between the nPDL and the organic layer yields a larger PC effect on the enhancement factor of the optical efficiency. When the material of the nPDL has a very high or very low refractive index compared with the organic materials, the enhancement factor and the enhanced wavelength peak change, as shown in **Figure S5**, indicating that the PC effect can no longer be ignored.

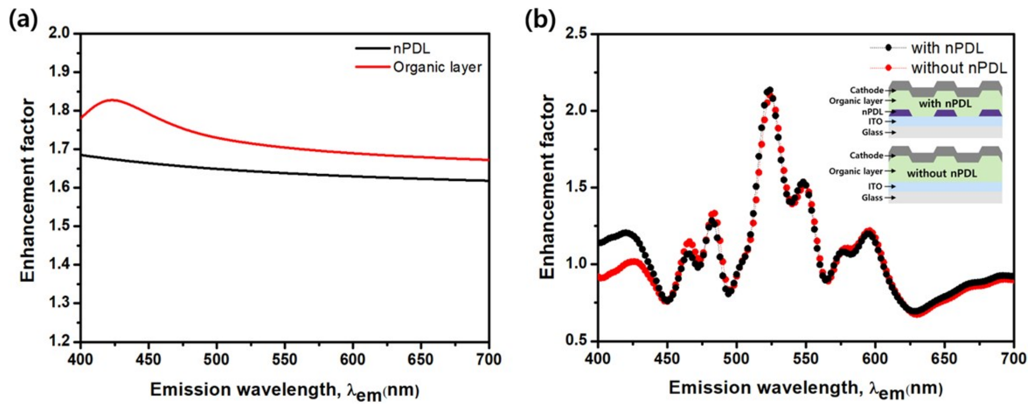

Figure S4. (a) Refractive indices of the nPDL and the organic layer. (b) Enhancement factor of OLEDs with and without the nPDL.

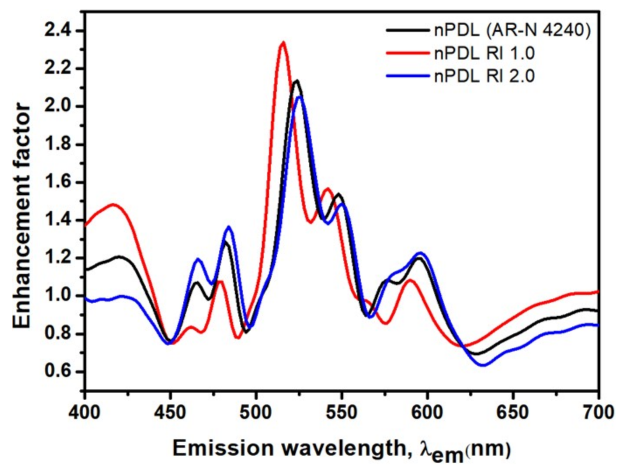

Figure S5. Enhancement factor–emission wavelength graph with respect to the refractive index of the nPDL difference.

2-2. Reduced SPP loss

Figure S6 shows the cross-sectional plane of the energy flux density from a vertical dipole (TM mode) in the conventional OLED and the nano-arrayed OLEDs with the nPDL. In the conventional structure shown in **Figure S6a**, the radiation is laterally confined to the organic–ITO layer (waveguide mode) or lost as it travels along the organic–metal interface (SPP mode), whereas in the nano-arrayed OLEDs shown in **Figures S6b and c**, the radiation confined as the SPP mode is reduced and extracted as an air mode owing to the periodic grating structure formed by the nPDL at the metal–organic interface. The periodic grating structure changes the wavevector of the confined SPP mode and allows it to radiate towards the substrate in both **Figure S6b** (without nPDL, but the periodic corrugation in the metal–organic interface remains) and **Figure S6c** (with nPDL).

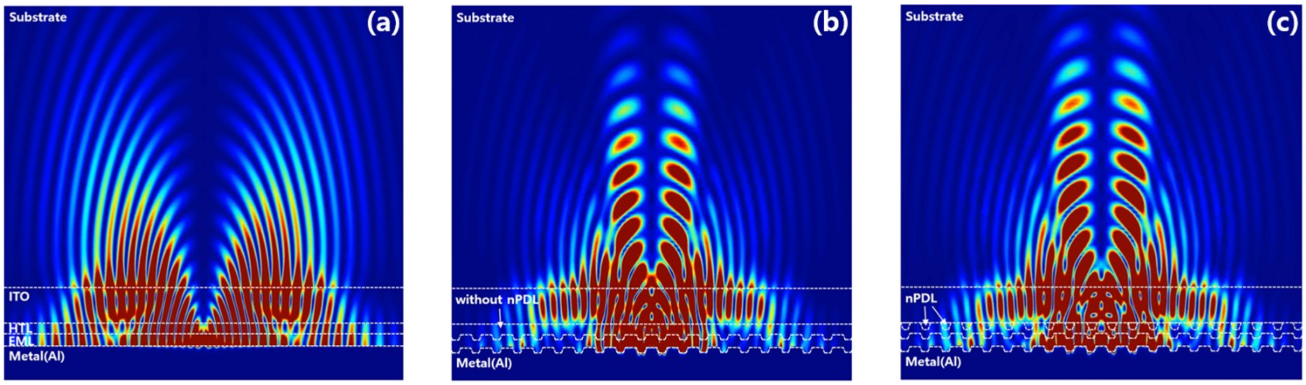

Figure S6. Energy flux density of the P-polarized dipole (TM mode) for (a) the conventional structure and (b) the nano-arrayed OLEDs without the nPDL and (c) with nPDL

To investigate the diffraction effect of the SPP mode in detail, we calculated the far-field intensity distribution with respect to the emission wavelength and angle, as shown in **Figure S7**. A deeper color represents a higher light intensity.

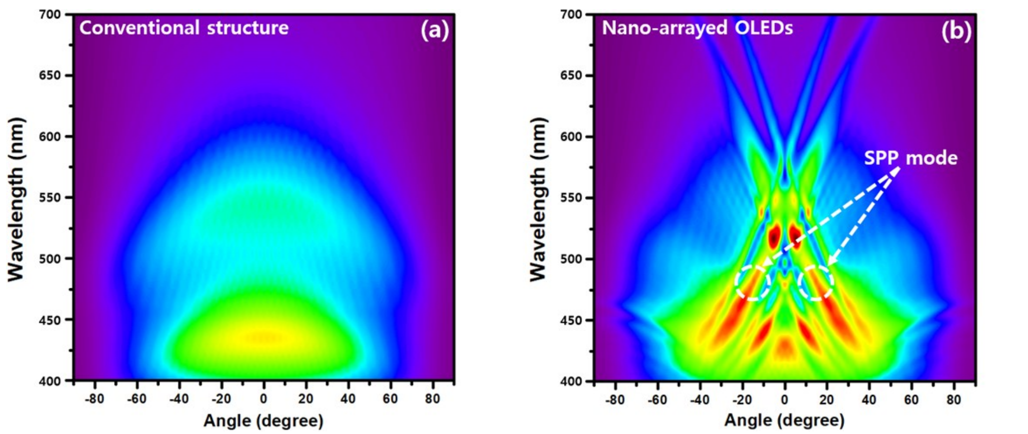

Figure S7. Far-field intensity angular distribution of (a) the reference device (b) the Nano-arrayed OLEDs

Compared with the far-field intensity distribution of the conventional OLED structure, the SPP diffraction patterns were observed in the nano-arrayed OLEDs. In nano-arrayed OLEDs, the far-field intensity is stronger than that for the conventional OLED in the green emission wavelength owing to the SPP diffraction (reduced SPP loss at the metal–organic interface), especially from the front viewing angle. This SPP diffraction pattern coincides with the calculation of the diffraction angle of the SPP mode as follows:

$$K_{spp} = \frac{2\pi}{\lambda}\sqrt{\frac{\varepsilon_m n_{org}^2}{\varepsilon_m + n_{org}^2}} = \frac{2\pi}{\lambda} n_g sin\theta_g \pm m\frac{2\pi}{\Lambda},$$

where m is the diffraction order, K_{spp} is wavevector of the SPP mode, λ is the emission wavelength, ε_m is the dielectric constant of the metal, n_{org} is the refractive index of the organic material, θ_g is the emissive angle, and ^ is the pitch of the corrugation pattern at the metal–organic interface (pitch of the nPDL).

In conclusion, the reduced SPP loss is the main cause of the enhanced optical efficiency of the nano-arrayed OLEDs considering the FDTD calculation and the negligible photonic crystal effect of the nPDL.

3. Electrical stability according to nPDL height

In the FDTD simulation data shown in **Figure 3b**, the optical-enhancement factor tends to increase with the height of the nPDL, up to a certain height. However, in the actual experiment data shown in **Figures S8a and b**, when the height of the nPDL exceeds 35 nm, the electrical characteristics of the device are unstable (electrical short of the device or decrease of the current density caused by the development of the photoresist), and the EQE decreases sharply. For these reasons, the height of the nPDL was set as 30–40 nm.

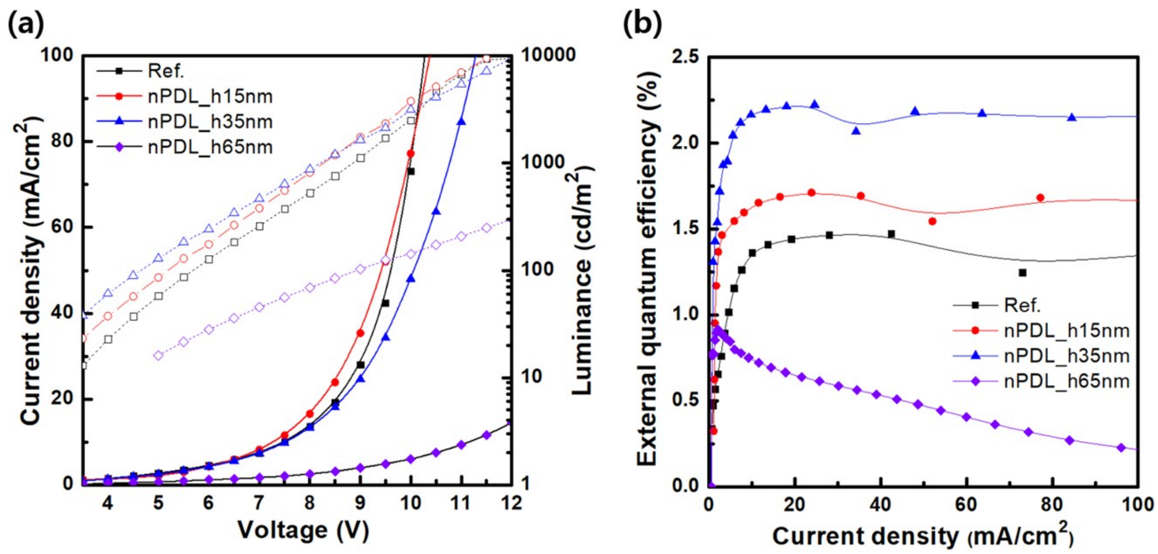

Figure S8. EL characteristics of the reference device and the nano-arrayed OLEDs with different heights. (a) Current density and luminance with respect to the voltage. (b) EQE with respect to the current density.

To reveal the effect of the nPDL height, simple fluorescent OLEDs were fabricated as follows:

[REF]

Glass / ITO / NPB (60 nm) / Alq_3 (80nm) / LiF / Al

[nPDL OLED]

Glass / ITO / nPDL / NPB (60 nm) / Alq_3 (80nm) / LiF / Al

4. Angular characteristics of nano-arrayed OLEDs

Figure S9 shows the angular characteristics of the nano-arrayed OLEDs. The nano-arrayed OLEDs exhibited spectrum distortion at 0° direction compared with the spectrum of the reference device because of the diffraction grating at the metal–organic interface. While the diffraction grating reduces the SPP loss at the metal–organic interface by changing the momentum of the SPP, it changes the spectrum according to the viewing angle.

Even though the spectrum of the nano-arrayed OLEDs differs from the reference at 0°, the CIE' 1931 color coordinates change little. This is because spectral changes (525-nm and 550-nm peaks in nano-arrayed OLEDs) have little effect on the color coordinates considering the spectrum of the devices and the color-matching function. As the viewing angle increases, the 550-nm peak at 0° is blue-shifted or red-shifted and decreases in intensity, making the spectrum almost identical at 60°.

As a result, the variation of the CIE' 1931 color coordinates at different emission angles is similar to that for the reference device.

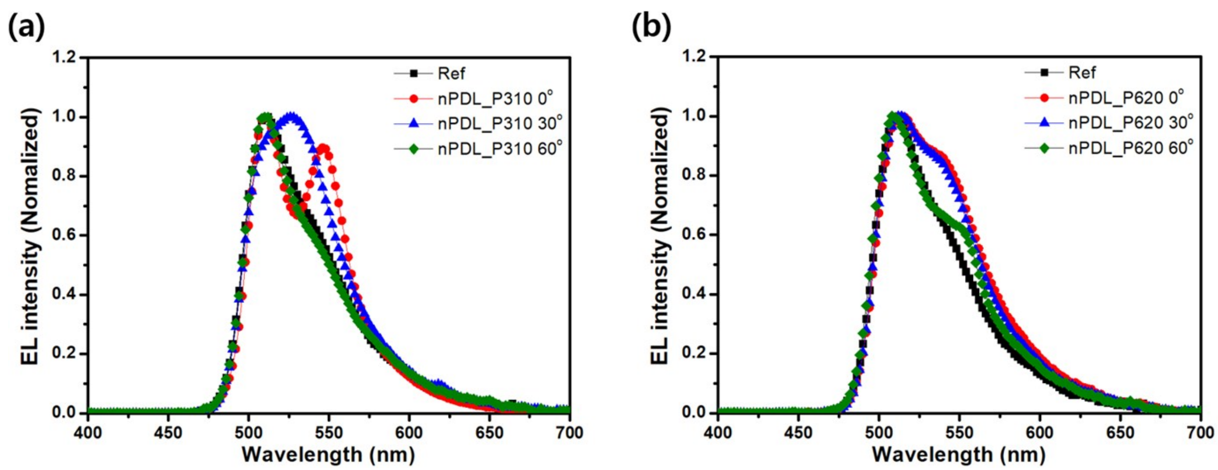

Figure S9. Angular dependence of the EL spectra: (a) the reference device and the nano-arrayed OLEDs with pitches of 310 nm and (b) the reference device and the nano-arrayed OLEDs with pitches of 620 nm.

5. Calculation of current density of nanopixels

From a physical viewpoint, as the ITO anode is covered with the nPDL (nanoholes), the current flow is limited to the pixel-defined area, excluding the part insulated by the nPDL. The current is highly concentrated in this region; thus, to investigate the physical roll-off characteristics of the nano-arrayed OLEDs, the current density was corrected considering the area of the actual current flow region (FF).

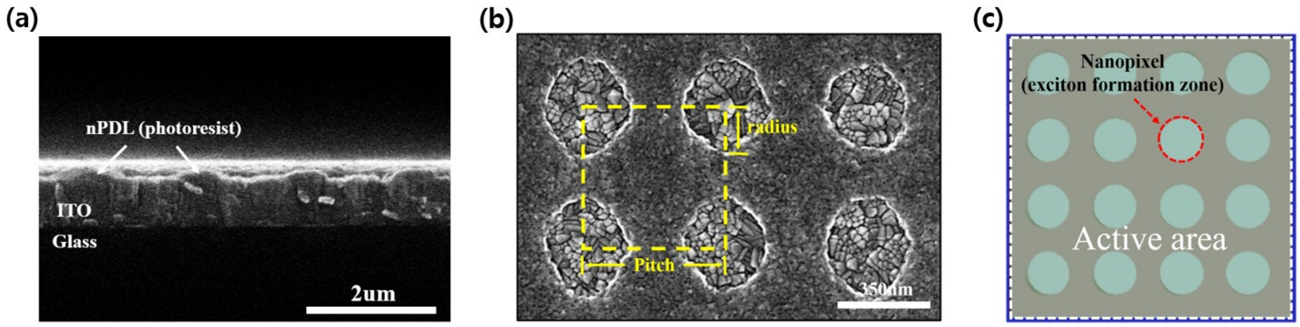

Figure S10. SEM image of the nPDL (a) cross-sectional view (b) top view. (c) Active area and nanopixels in the nano-arrayed OLEDs.

The pitch and the FF of the nPDL were determined as follows:

$$\text{pitch} = \frac{\lambda_{\text{Ar}}}{2\sin\theta}$$

$$\text{fill factor} = \frac{\pi \times (\text{radius of nanohole})^2}{\text{pitch}^2},$$

where λ_{Ar} is the wavelength of the Ar-ion laser, and θ is the incident angle of light on the Lloyd's interferometer mirror.

The current density of the nanopixels was defined as the measured current divided by the active area and the FF, as follows:

$$current\ denstiy\ of\ nanopixels = \frac{measure\ current}{active\ area\ \times FF}$$
$$= \frac{measured\ current\ density}{FF}.$$

The current was measured using a Keithley 237 unit. The actual current flow region is the product of the active area ($6.25\ mm \times 6.25\ mm$) and the FF (which is 1.0 for the reference device).

Table 2. Current density of nanopixels

	measured current density	FF0.05	FF0.1	FF0.15	FF0.25
current density of nanopixels	1	20	10	6.66	4

6. Critical current density of nanopixels

The maximum EQE in nano-arrayed OLEDs with different FFs were slightly different because of nano-optical effects. For direct comparison of the critical current densities, in the Supporting

Information, we added the normalized EQE (a.u.) with respect to the current density of the nanopixels. The maximum EQE value of each devices is equal to 1.0.

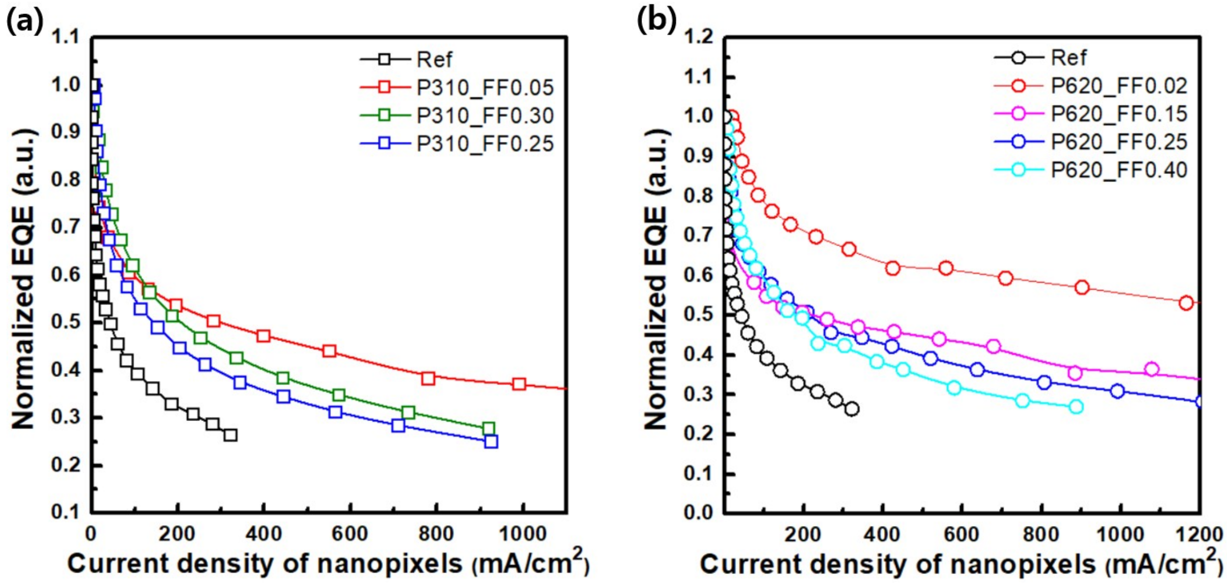

Figure S11. Normalized EQE with respect to the current density of nanopixels (a) with pitches of 310 nm and (b) with pitches of 620 nm.

7. Red and Blue emission Nano-arrayed OLEDs

To verify the practicability of the nPDL, red and blue emission nano-arrayed OLEDs were fabricated. The nPLD with the pitch of 380nm and 460nm were inserted for red and blue OLEDs, respectively. Their configurations are as follows:

[Ref-Red]

Glass / ITO / NPB (40 nm) / TCTA (10 nm) / CBP: PQ_2Ir (30 nm) / B3PyMPM (55 nm) / LiF / Al

[nPDL-Red]

Glass / ITO / nPDL (380 nm-pitch) / NPB (40 nm) / TCTA (10 nm) /
CBP: PQ_2Ir (30 nm) / B3PyMPM (55 nm) / LiF / Al.

[Ref-Blue]

Glass / ITO / NPB (40 nm) / TCTA (10 nm) / CBP: FIrpic (30 nm) / B3PyMPM (55 nm) / LiF / Al

[nPDL-Blue]

Glass / ITO / nPDL (460 nm-pitch) / NPB (40 nm) / TCTA (10 nm) /
CBP: FIrpic (30 nm) / B3PyMPM (55 nm) / LiF / Al.

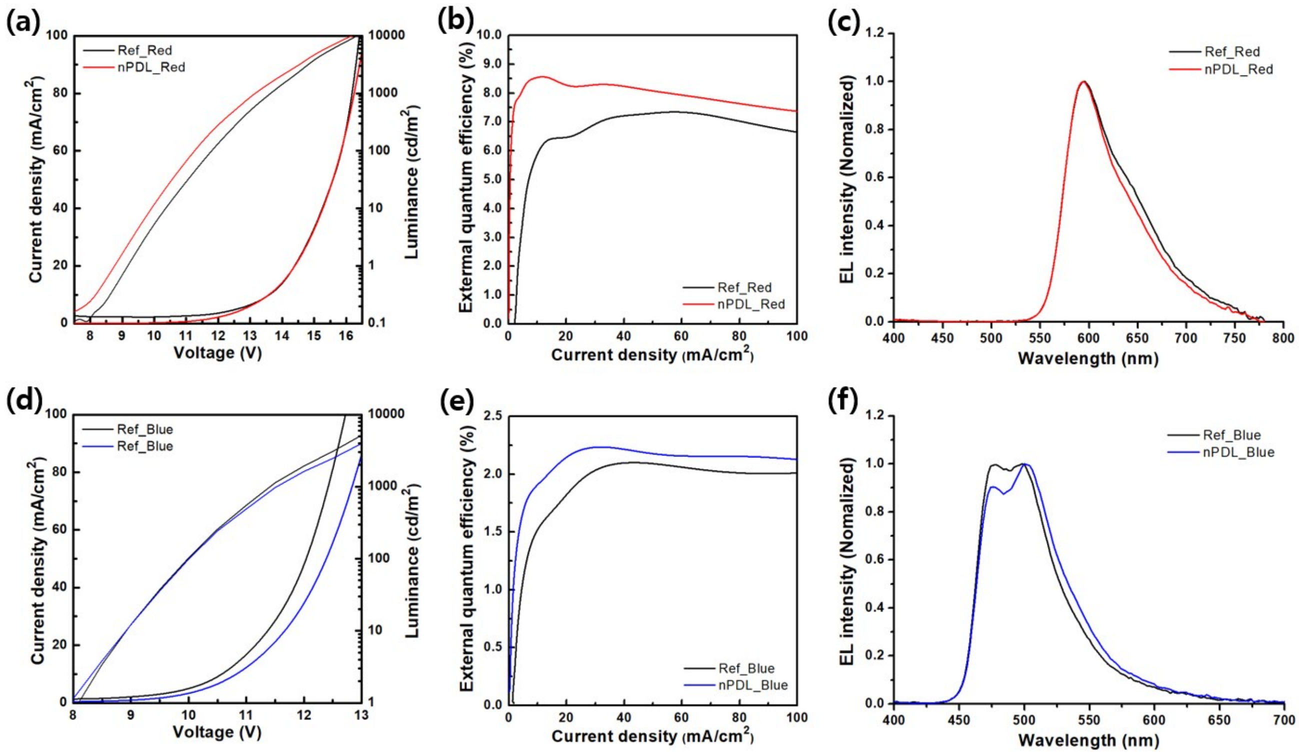

Figure S13. EL characteristics of Red emission OLEDs. **(a)** JVL curve **(b)** EQE with respect to current density **(c)** Normalized EL intensity EL characteristics of Blue emission OLEDs. **(d)** JVL curve **(e)** EQE with respect to current density **(f)** Normalized EL intensity

Although the carrier balance is not optimized in these experimental OLEDs, the improvement of EL characteristics found in green emission OLEDs were equally found in the red and blue emission OLEDs. The EQE of nPDL_Red and Blue devices were improved by 40.87% and 10.15%, respectively, at 1000 cd/m^2 compared to the reference device.